Correlated fermions on a checkerboard lattice

Frank Pollmann,[1] Joseph J. Betouras,[2,3] Kirill Shtengel,[4] and Peter Fulde[1]

[1]*Max-Planck-Institute for the Physics of Complex Systems, D-01187 Dresden, Germany*
[2]*Instituut-Lorentz for Theoretical Physics, P.O. Box 9506, NL-2300RA Leiden, The Netherlands*
[3]*School of Physics and Astronomy, Scottish Universities Physics Alliance, University of St Andrews, North Haugh KY16 9SS, UK*
[4]*Department of Physics and Astronomy, University of California, Riverside, CA 92521, USA*

(Dated: February 6, 2008)

A model of strongly correlated spinless fermions on a checkerboard lattice is mapped onto a quantum FPL model. We identify a large number of fluctuationless states specific to the fermionic case. We also show that for a class of fluctuating states, the fermionic sign problem can be gauged away. This claim is supported by numerical evaluation of the low-lying states. Furthermore, we analyze excitations at the Rokhsar-Kivelson point of this model using the relation to the height model and the single-mode approximation.

The interplay between quantum and geometric frustration can result in many unusual properties. From that point of view, strongly correlated spinless fermions on a checkerboard lattice present an interesting case. At certain fillings, fractionally charged excitations have been predicted for the case of large nearest-neighbor repulsion [1]. The subject is not purely academic since the checkerboard lattice is a projection of a pyrochlore lattice onto a plane. There is experimental evidence that electrons in pyrochlore lattices can be strongly correlated [2]. We shall show that at half filling, this problem can be mapped onto a quantum fully packed loop (FPL) model – an analog of the quantum dimer model (QDM) – and discuss a number of consequences. QDMs, originally introduced in the context of quantum magnetism [3], became a focus of recent interest following the discovery of a gapped liquid phase on a triangular lattice [4]. In particular, it has been established that a gapped phase with deconfined excitations exists in 2D for QDMs on non-bipartite lattices [4, 5, 6, 7] while on bipartite lattices, such as a square lattice, systems typically crystallize into a phase with a broken translation/rotation symmetry. The liquid phase is "shrunk" into a quantum critical point with gapless excitations [3, 8, 9]. In both cases, an effective gauge theory is a U(1) theory for such a critical point and a Z_2 theory for a deconfined phase [10, 11]. Several related models, such as the quantum six/eight-vertex models [12, 13, 14, 15] have been shown to conform to the same dichotomy: a model with orientable loops is critical and is described by a U(1) gauge theory.

The aforementioned models share one important feature: the matrix elements connecting various states of the low-energy Hilbert space are all non-negative. The Hilbert space separates into different sectors so that all states within a sector are connected by the quantum dynamics while states belonging to different sectors are not. Then, by Perron-Frobenius theorem, the ground state (GS) of each sector is unique and nodeless [4, 16]. Much less is known about models with non-Frobenius dynamics which results in some negative matrix elements. A striking difference between Frobenius vs. non-Frobenius QDMs on the kagomé lattice was found in [7, 17]: while the conventional QDM exhibits a gapped Z_2 topological phase, its counterpart with different signs has an extensive GS degeneracy. A different non-Frobenius model of lattice fermions [18] has also been found to have an extensive GS degeneracy.

The starting Hamiltonian for spinless fermions is:

$$H = -t \sum_{\langle i\, j\rangle} \left(c_i^\dagger c_j + \text{H.c.} \right) + V \sum_{\langle i\, j\rangle} n_i n_j, \qquad (1)$$

the summation is over neighboring sites of a checkerboard lattice. We assume that $0 < t \ll V$ – the limit of strong correlations. At half-filling which is studied here, the potential term is minimized whenever there are two fermions on each "planar tetrahedron", i.e., a crisscrossed square in Fig. 1(a) (the tetrahedron rule, [19]). Configurations satisfying this rule can be represented by dimers on a square lattice connecting the centers of the planar tetrahedra, with the particles sitting in the middle of the dimers (Fig. 1(a)) [20]. Hence, the states satisfying the tetrahedron rule are represented by non-intersecting FPL on the square lattice. Different loop configurations are orthogonal to each other as they correspond to different locations of fermions (in the tight-binding limit, the overlap between the corresponding wavefunctions is neglected).

We now turn our attention to the kinetic term in Hamiltonian (1). It creates configurations in which the tetrahedron rule is violated. But since we are interested in the low-energy physics we may eliminate these configurations and consider instead an effective ring-exchange Hamiltonian [21] that acts *within* the FPL Hilbert subspace. To lowest non-vanishing order in t/V, such effective Hamiltonian becomes:

$$H_{\text{eff}} = g \sum_{\{\square,\square\}} \Big(|\square\rangle\langle\square| + \text{H.c.} \Big) - g \sum_{\{\square,\square\}} \Big(|\square\rangle\langle\square| + \text{H.c.} \Big)$$
$$\equiv g \sum_p \Big(|A\rangle\langle\overline{A}| + |\overline{A}\rangle\langle A| - |B\rangle\langle\overline{B}| - |\overline{B}\rangle\langle B| \Big) \qquad (2)$$

where the sums are performed over all polygons of perimeter six and $g = 12t^3/V^2$. Particles are located in the middle of the dimers. The different signs result from the number of permuted fermions which is either even or odd.

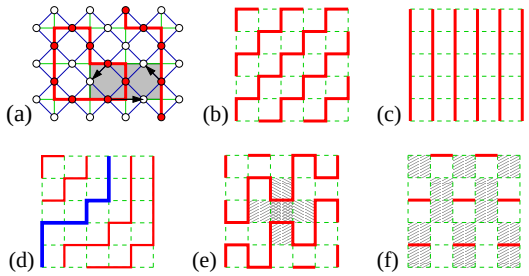

FIG. 1: (a) – A configuration of fermions satisfying the "two per tetrahedron" rule and its representation in terms of FPLs. A smallest "flippable plaquette" is shaded (see text for details). (b–d) – Fragments of possible "frozen" states: (b) is fluctuationless under *any* local ring exchanges while (c) and (d) are fluctuationless only for fermionic ring exchanges. (e) – The long-range ordered "squiggle" state maximizing the number of three-dimer ring exchanges (shaded). (f) – Analog of a plaquette phase, with three dimers predominantly fluctuating around shaded rectangles, shown dimers are not participating in these exchanges.

Symmetries and Conserved Quantities – The first important point is that this model is a variation of the quantum six-vertex (6V) model [12, 14, 15] [29]. However, there are two important differences resulting from the fermionic statistics. Firstly, only ring exchanges involving *odd numbers* of particles are allowed; the contributions from clock- and counter-clockwise ring moves of an even number of fermions cancel. In particular, the smallest resonating plaquette has perimeter six, rather than four, as captured by Eq. (2). Secondly, the sign of the ring-hopping term depends on the occupancy of the middle bond. Both differences have important implications: the first one – for the ergodicity of the quantum dynamics, while the second one leads to a sign problem in the quantum Monte Carlo dynamics.

Let us now discuss symmetries and conservation laws pertaining to our model. Firstly, since its Hilbert space is equivalent to that of a 6V model, it has a height representation [22]. The quantum dynamics can also be described in the height language [23, 24]. The immediate consequence is that *no* such local dynamics can change the global slopes $\kappa_x(y)$ and $\kappa_y(x)$ in x and y directions, which therefore form a set of conserved numbers. Additionally, there is an accidental symmetry in our model, specific to the quantum dynamics (2): it conserves the total numbers of both vertical and horizontal dimers (moreover, it conserves the number of horizontal dimers in even and odd rows separately, and similarly for the vertical dimers). Hence, all states can be classified with respect to these quantum numbers which are *different* from the aforementioned conserved slopes. Notice that these additional conservation laws will not survive if higher-order ring-exchange terms are added to the Hamiltonian (2).

Sign Problem – The sign problem manifested in the opposite signs of the $A \leftrightarrow \overline{A}$ and $B \leftrightarrow \overline{B}$ terms in Eqs. (2) can be avoided in certain (but not all) cases. Notice that $B \leftrightarrow \overline{B}$ processes do not change the loop topology (or their number), while the $A \leftrightarrow \overline{A}$ flips always do, with the possibilities presented schematically in Fig. 2(a). Let us consider the coarse-grained surface with an even number of fermions remaining fixed at the boundary ("fixed" boundary conditions (BC)). Then fermion configurations are represented by closed loops as well as arcs terminating at the boundary. With no fermions at the boundary, there are closed loops only (Fig. 2(b)), which we orient as follows: (i) color the areas separated by the loops white and grey, with white being the outmost color; (ii) orient all loops so that the white regions are always to the right. In the presence of arcs (Fig. 2(c)) we can choose how to close them on the outside without intersections (the outside region has no dynamics). Letting white be the color at infinity, we orient the loops as described above. We now notice that the relative signs resulting from the $A \leftrightarrow \overline{A}$ flips are consistent with multiplying each loop configuration by $i^l(-i)^r$, where r (l) is the number of the (counter-) clockwise winding loop Hence, by simultaneously changing the sign of the $A \leftrightarrow \overline{A}$ flips and transforming the loop states $|\mathcal{L}\rangle \to i^{l(\mathcal{L})}(-i)^{r(\mathcal{L})}|\mathcal{L}\rangle$, we cure the sign problem thus making the system effectively bosonic. (In fact, this fix can be related to a more general class of gaugeable signs discussed in [16].)

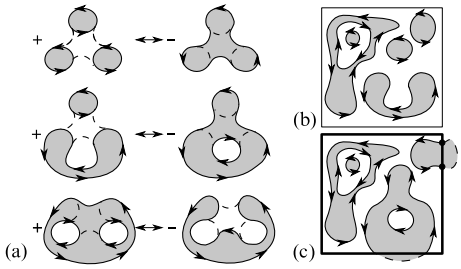

FIG. 2: (a) Three different actions of the effective Hamiltonian on the topology of loop configurations. (b, c) Representation of configuration as fully-packed directed loops.

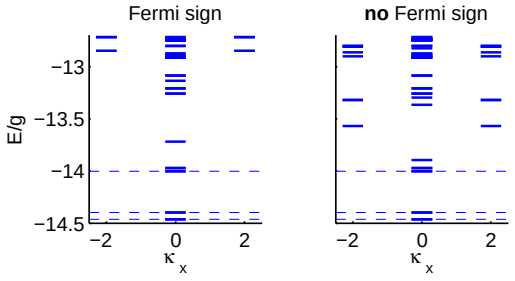

FIG. 3: GS energy and energies of lowest excited states of the effective Hamiltonian in sectors with different slopes (κ_x, 0). Left panel: Data from an exact diagonalization of H_{eff} on a 72 site cluster where the Fermi sign is taken into account. Right panel: Same data from a calculation with excluded Fermi signs.

Note that this construction need not work for the periodic BC: firstly, only even-winding sectors on a torus allow two-coloring, and secondly, even for even windings, it is possible to dynamically reverse the coloring while returning to the same loop configuration, resulting in non-trivial state count-

ing. It appears though that for the periodic BC on *even* tori (preserving the bipartiteness of the lattice), the lowest-energy states belong to the sector where such transformation works, as confirmed by the exact diagonalization results (Fig. 3). The presented non-local loop-orienting construction is restricted to the ring-exchange processes of length six.

Rokhsar-Kivelson (RK) Point – It has been shown that at half-filling the Hamiltonian (2) has an ordered GS and fractionally charged, weakly confined excitations [25]. In the spirit of [3], we extend our model's parameter space in order to study its phase diagram and consider the Hamiltonian

$$H'_{\text{eff}} = \sum_p \big[g \left(|A\rangle\langle\overline{A}| + |\overline{A}\rangle\langle A| - |B\rangle\langle\overline{B}| - |\overline{B}\rangle\langle B| \right) + \mu \left(|A\rangle\langle A| + |\overline{A}\rangle\langle\overline{A}| + |B\rangle\langle B| + |\overline{B}\rangle\langle\overline{B}| \right) \big] \quad (3)$$

where we use the short-hand notations introduced in Eq. (2). At the RK point $g = \mu$, this Hamiltonian can be written as a sum of projectors:

$$H'_{\text{eff}}|_{g=\mu} = g \sum_p \big[\left(|A\rangle + |\overline{A}\rangle \right) \left(\langle A| + \langle\overline{A}| \right) + \left(|B\rangle - |\overline{B}\rangle \right) \left(\langle B| - \langle\overline{B}| \right) \big] . \quad (4)$$

A (non-unique) GS of Hamiltonian (4) is a state that is annihilated simultaneously by all projectors. There are two kinds of such states: *frozen* states and *liquid* states. It turns out that the fermionic nature has strong consequences for both kinds. All bosonic frozen states identified in [13] remain frozen since they are unaffected by *any* local ring exchange. In the height language, these states maximize the slope in either x or y direction, making any local dynamics impossible. Fixing this slope in an $L \times L$ system, one still has 2^L possible arrangements of steps in the other direction which results in 4×2^L such states [30]. However, there are also new additional GSs (see Fig. 1(c,d)) which remain unaffected by any *fermionic* dynamics but would not be so in the bosonic case. This is due to the fact that only odd-fermion ring exchanges are allowed here. For the types of states shown in Fig. 1(c,d), this is easy to see: any ring exchange is an alternating sequence of occupied and vacant bonds. The subsequence of vacant bonds maps onto a 1D walk between the lines and must contain an *even* number of steps in order to close. The states of this type are obtained by translating a single line like in Fig. 1(d), e.g., a line starting at the left bottom corner $(0, 0)$ and reaching the top boundary at (x, L) while going only up and to the right (we assume free BC) can do it in $\binom{L+x}{x}$ distinct ways leading to $4 \times \sum_{x=0}^{L} \binom{L+x}{x} \to 4^{L+1}$ (for large L) such frozen fermionic states. There is also a number of other frozen fermionic configurations that we could pinpoint (but not systematically count). Hence it remains an open issue whether our RK point is characterized by an extensive GS entropy and whether such entropy observed in [17, 18] can be explained in this manner. However, it is very suggestive that the explanation lies in a more restrictive nature of the fermionic dynamics. We stress that these "new" frozen GSs are not related to any height constraints – in fact, the states of type shown in (Fig. 1(d)) include both the maximally tilted state (Fig. 1(b)) and the maximally flat state (Fig. 1(c)). "Freezing" of the latter state is especially interesting since it is supposed to dominate the ordered phase of the bosonic model for $\mu/g < -0.374$ [13] by maximizing the number of the flippable plaquettes [31]. This observation puts into doubt the existence of such a phase in the fermionic model.

In addition to the frozen states, there are also liquid-like GSs, as was the case in the original RK construction. These states can be found exactly for the dynamics given by Eqs. (2–4) with the help of the aforementioned sign-fixing transformation. (While this transformation changes the sign of the $A \leftrightarrow \overline{A}$ flips, it does not affect the diagonal terms in Eqs. (3).) Hence, for "fixed" BC, the state $|0\rangle \propto \sum_{\{\mathcal{L}\}} i^{l(\mathcal{L})}(-i)^{r(\mathcal{L})}|\mathcal{L}\rangle$ is automatically annihilated by all projector terms in $H_{\text{eff}'}$ and therefore is a GS. Here the sum is taken over all loop configurations $\mathcal{L}$ that are connected to each other by the quantum dynamics. Note that there are many disconnected sectors.

Excitations at the RK point – The quantum dynamics of the Hamiltonian H_{eff} and similarly H'_{eff} can be described in terms of a height model [23, 24]. The associated conserved quantities κ_x and κ_y, as well as their insensitivity to a constant shift of the height field imply gapless hydrodynamic modes with $\omega(k) \sim k^2$ as $k \to 0$. The liquid state of the FPL model at the RK point corresponds to the rough phase of the height model, in which case the modes can be identified as the so-called resonons at wavevector (π, π) [3] and the equivalent of the pi0ns, here at $\mathbf{Q} = (0, 0)$ [26, 27, 28].

For constructing gapless excitations in our model, we adopt the single-mode approximation which has been successfully used for the QDM on the square lattice [3, 28]. Let $|0\rangle$ be the aforementioned "liquid" GS at the RK point. The operator $d^{\pm}_{\hat{\tau}}(\mathbf{r})$ creates (annihilates) a dimer at position $\mathbf{r}$ in direction $\hat{\tau}$. The density operator $n_{\hat{\tau}}(\mathbf{r}) = d^{+}_{\hat{\tau}}(\mathbf{r}) d^{-}_{\hat{\tau}}(\mathbf{r})$ has the Fourier transform $n_{\hat{\tau}}(\mathbf{q}) = \sum_{\mathbf{r}} n_{\hat{\tau}}(\mathbf{r}) \exp(i\mathbf{q} \cdot \mathbf{r})$. We use the operators $n_{\hat{\tau}}(\mathbf{q})$ to construct the states $|\mathbf{q}, \hat{\tau}\rangle = n_{\hat{\tau}}(\mathbf{q})|0\rangle$ which are for $\mathbf{q} \neq 0$ orthogonal to $|0\rangle$. The excitation energies are bounded by $E(\mathbf{q}, \hat{\tau}) \leq f(\mathbf{q})/S_{\tau\tau}(\mathbf{q})$, where $f(\mathbf{q}) = \langle 0|[n_{\hat{\tau}}(-\mathbf{q}), [H'_{\text{eff}}, n_{\hat{\tau}}(\mathbf{q})]]|0\rangle$ is the the oscillator strength and $S_{\tau\tau}(\mathbf{q}) = \langle 0|n_{\hat{\tau}}(-\mathbf{q}) n_{\hat{\tau}}(\mathbf{q})|0\rangle$ is the structure factor. In order to calculate $f(\mathbf{q})$, we observe that the density operators commute with the potential energy term, hence only the kinetic energy term contributes. By using the commutation relation $[d^{\pm}_{\hat{\tau}}, n_{\hat{\tau}}] = \mp d^{\pm}_{\hat{\tau}}$ repeatedly, we compute $f(\mathbf{q})$ due to the resonating terms for $\hat{\tau} = \hat{x}$. The upshot is that to leading order $f(\mathbf{k}) \sim (\mathbf{k} \times \hat{\tau})^2$ (similar type of expression as the one for the RK model [3]) with $\mathbf{k} = \mathbf{q} - \mathbf{Q}$ at $\mathbf{Q} = (0, 0), (\pi, \pi), (0, \pi)$. The second ingredient, the structure factor $S_{xx}(\mathbf{q})$ is the Fourier transform of the dimer density correlation function. We use the expression given in Ref. [27] for it. Interestingly, $S_{xx}(\mathbf{q}) \neq 0$ except along the direction $\mathbf{q} = (q_x, \pi)$ where it vanishes with the exception of (π, π). At $(0, \pi)$ both $f(\mathbf{q})$ and $S_{xx}(\mathbf{q})$ are zero, but their ratio remains finite. In addition $S_{xx}(\mathbf{q})$ shows no singularities. The FPL model differs from the hardcore dimer model

(describing our model at quarter-filling) for which $S_{xx}(\mathbf{q})$ diverges logarithmically at $\mathbf{Q} = (\pi, 0)$ [28]. The difference is due to a slower algebraic decrease with distance of the correlation function for hardcore dimer covering. We have also verified the above result for our structure factor $S_{xx}(\mathbf{q})$ by means of Monte Carlo simulations.

We conclude with several observations and open questions addressing the possible phase diagram of the model defined by Eq. (3). The bosonic version studied in [13] has three phases depending on the parameter μ/g: the two "flat" phases, i.e., the Néel phase [13] and the plaquette phase (also found in [14, 27]) as well as a maximally tilted frozen phase, with the RK point perched between the latter two phases. We have already argued that some of the flat states are actually frozen for fermions and hence cannot be used to define the fluctuation-stabilized phases for $\mu/g < 1$. The nature, and number of such phases are an open question, but let us attempt an analysis. Firstly, the maximally-flat (Néel, DDW) phase shown in Fig. 1(c) appears to be replaced by the somewhat analogous "squiggle" phase (Fig. 1(e))[25]. In the bosonic case, the region of $-0.374 < \mu/g < 1$ corresponded to the plaquette phase, while its direct fermionic analog does not appear to be present anywhere in the fermionic phase diagram. (Notice, however, that unlike the Néel and the plaquette phases, both states shown in Fig. 1(e,f) break *both* translation and rotation symmetries simultaneously.) We rule this phase out based on the fact that the squiggle phase breaks the symmetry between the numbers of the vertical and the horizontal dimers (which are separately conserved by the quantum dynamics), while the "fermionic plaquette" phase does not. The results of the exact diagonalization on the small samples indicate that this symmetry remains broken all the way up to $\mu/g = 1$ – the RK point, with the ratio of 2/3 being consistent with the "squiggle" phase. This observation is also strongly disfavoring a critical liquid phase to the left of the RK point, hence the fermionic RK point in this model is likely to be an isolated quantum critical point just as it is for the bosonic model. The gapless modes identified above are in agreement with such a scenario. The details of the phase diagram and its sensitivity to the higher order ring exchanges is a subject for future work.

The authors would like to thank R. Moessner and E. Runge for many illuminating discussions. F. P. has benefited from the hospitality of IDRIS, Orsay during a stay made possible by a HPC Europe grant (RII3-CT-2003-506079). K. S. is grateful for the hospitality of the MPIPKS, Dresden and the Instituut-Lorentz, Leiden. While this paper was in preparation, we learned about a similar effort undertaken by C. Penc and N. Shannon.

[1] P. Fulde, K. Penc, and N. Shannon, Ann. Phys. (Leipzig) **11**, 892 (2002), cond-mat/0211034.

[2] S. Kondo, D. C. Johnston, C. A. Swenson, F. Borsa, A. V. Mahajan, L. L. Miller, T. Gu, A. I. Goldman, M. B. Maple, D. A. Gajewski, et al., Phys. Rev. Lett. **78**, 3729 (1997).

[3] D. S. Rokhsar and S. A. Kivelson, Phys. Rev. Lett. **61**, 2376 (1988).

[4] R. Moessner and S. L. Sondhi, Phys. Rev. Lett. **86**, 1881 (2001), cond-mat/0007378.

[5] C. Nayak and K. Shtengel, Phys. Rev. B **64**, 064422 (2001), cond-mat/0010242.

[6] P. Fendley, R. Moessner, and S. L. Sondhi, Phys. Rev. B **66**, 214513 (2002), cond-mat/0206159.

[7] G. Misguich, D. Serban, and V. Pasquier, Phys. Rev. Lett. **89**, 137202 (2002), cond-mat/0204428.

[8] R. Moessner and S. L. Sondhi, Phys. Rev. B **68**, 184512 (2003), cond-mat/0307592.

[9] E. Fradkin, D. A. Huse, R. Moessner, V. Oganesyan, and S. L. Sondhi, Phys. Rev. B **69**, 224415 (2004), cond-mat/0311353.

[10] E. Fradkin and S. A. Kivelson, Mod. Phys. Lett. B **4**, 225 (1990).

[11] R. Moessner, S. L. Sondhi, and E. Fradkin, Phys. Rev. B **65**, 024504 (2001), cond-mat/0103396.

[12] E. Ardonne, P. Fendley, and E. Fradkin, Ann. Phys **310**, 493 (2004), cond-mat/0311466.

[13] N. Shannon, G. Misguich, and K. Penc, Phys. Rev. B **69**, 220403(R) (2004), cond-mat/0403729.

[14] O. F. Syljuasen and S. Chakravarty, Phys. Rev. Lett. **96**, 147004 (2006), cond-mat/0509624.

[15] S. Chakravarty, Phys. Rev. B **66**, 224505 (2002), cond-mat/0206282.

[16] C. Castelnovo, C. Chamon, C. Mudry, and P. Pujol, Ann. Phys. **318**, 316 (2005), cond-mat/0502068.

[17] G. Misguich, D. Serban, and V. Pasquier, Phys. Rev. B **67**, 214413 (2003), cond-mat/0302152.

[18] P. Fendley and K. Schoutens, Phys. Rev. Lett. **95**, 046403 (2005), cond-mat/0504595.

[19] P. W. Anderson, Phys. Rev. **102**, 1008 (1956).

[20] F. Pollmann, J. J. Betouras, and E. Runge, Phys. Rev. B **73**, 174417 (2006), cond-mat/0604669.

[21] E. Runge and P. Fulde, Phys. Rev. B **70**, 245113 (2004).

[22] H. van Beijeren, Phys. Rev. Lett. **38**, 993 (1977).

[23] C. L. Henley, J. Stat. Phys. **89**, 483 (1997), cond-mat/9607222.

[24] C. L. Henley, J. Phys.: Condens. Matter **16**, S891 (2004), cond-mat/0311345.

[25] F. Pollmann and P. Fulde, Europhys. Lett. **75**, 133 (2006), cond-mat/0604666.

[26] R. Moessner and S. L. Sondhi, Phys. Rev. B **68**, 064411 (2003), cond-mat/0303210.

[27] R. Moessner, O. Tchernyshyov, and S. L. Sondhi, J. Stat. Phys. **116**, 755 (2004).

[28] R. Moessner and S. L. Sondhi, Phys. Rev. B **68**, 184512 (2003), cond-mat/0307592.

[29] The mapping between FPL and 6V is done by subdividing the square lattice into even and odd sublattices and orienting occupied bonds from odd to even sites, with the opposite orientation for vacant bonds.

[30] This is unlike the QDM case with only 4 such frozen, or *staggered* states: maximizing the slope in one direction there automatically fixes it in the other.

[31] This is the conventional anti-ferroelectric phase of the six-vertex model referred to as the Néel phase in [13] and as DDW phase in [14, 15]